Granular Matter (2015) 17:377–387
DOI 10.1007/s10035-015-0557-1

ORIGINAL PAPER

Discrete element cluster modeling of complex mesoscopic particles for use with the particle flow code method

Chong Shi[1,2] · **De-jie Li**[1,2] · **Wei-ya Xu**[1,2] · **Rubin Wang**[1,2]

Received: 11 December 2014 / Published online: 29 March 2015
© Springer-Verlag Berlin Heidelberg 2015

Abstract Based on the configuration principle of the discrete element method, local Delaunay mesh, and distance control the method, the overlapping discrete element cluster, non-overlapping discrete element cluster are employed to model mesoscopic geotechnical particles using discrete elements comprised of disks (or spheres). A kinetic compatibility procedure is established for adjusting the disk (or sphere) densities. Based on overlapping discrete element cluster modeling method, a new method, named boundary filling discrete element cluster method, has been put forward. The applicability of each method is considered by means of a numerical experiment. Of the three methods laboratory test considered, the boundary filing discrete element cluster modeling method demonstrated the highest calculation efficiency, followed by the overlapping discrete element cluster modeling method. Relative to these methods, the non-overlapping discrete element cluster modeling method is applicable to simulation of the deformation and fracture of particles, although the method demonstrates lower computational efficiency. All three methods can be readily applied to three-dimensional cases; thus, the discussed modeling methods will be beneficial in the field of mesoscopic analysis of geo-materials.

Keywords Mesoscopic medium · Particle shape characterization · Overlapping discrete element cluster · Deformation discrete element cluster · Boundary filing discrete element clusters

1 Introduction

The mechanical properties of geomaterials are influenced by mesoscopic characteristics such as particle size, gradation, outer contour, and roughness. To analyze the characteristics of deformation and strength, experiments are typically conducted to study the relationships among particle size, gradation, and mechanical properties. Recently, with the development of analysis methods for evaluating mesoscopic characteristics, particle surface characterization methods have received increasing attention.

With the application and development of the discrete element method (DEM), computational research into the mechanical properties of materials with consideration for mesoscopic characteristics has achieved substantial progress [1–5]. For example, DEM simulation using the particle flow code (PFC) package adopts discrete elements comprised of disks (or spheres) or multiple bonded disks (or spheres) to form clusters, and then simulates the mechanical properties of granular matter. However, it is difficult to construct a realistic particle with accurate mesoscopic characteristics such as outer contour, roughness, and texture by DEM [6–8].

To construct more realistic particle models, numerous scholars have proposed techniques to model irregularly shaped particles using discrete elements comprised of disks (or spheres), which are then bonded to form clusters. Presently, two main methods have been developed for constructing discrete element clusters: the dynamic method and the mathematical filling method. The dynamic method firstly

✉ Chong Shi
shichong81@126.com

[1] Key Laboratory of Ministry of Education for Geomechanics and Embankment Engineering, Hohai University, Nanjing 210098, China

[2] Institute of Geotechnical Research, Hohai University, Nanjing 210098, China

generates a series of small disks (or spheres) within the particle domain, and then the radii of the disks (or spheres) are progressively increased until the particle domain is filled out to the inner edge of the particle contour [9]. The mathematical filling method generates a series of disks (or spheres) within the contour of the particle domain according to some mathematical rules, and, through changing the radii of the discrete elements, a cluster is formed with various outlines, roughness, and texture [10].

Overlap between disks cannot be avoided in a cluster modeled by the dynamic method, and numerical simulations aimed at particle deformation and fracture result in a release of strain energy. Therefore, to obtain an ideal discrete element cluster model, expansion and dynamically iterative calculations are usually required [11,12]. However, the mathematical filling method can control the degree of overlap through the mathematical tangent condition between disks or spheres, making the iterative process unnecessary and resulting in a wider application purview.

In some certain conditions, particles can be regarded as rigid bodies, overlap between disks (or spheres) is allowed. Hereby this perspective, Yun [13] and Markauskas [14] combined disks according to linear superpositiona and proposed that irregular particles can be equivalent astreated as spherical or ellipsoidal particles by controlling the number and radii of disks. Based on DEM, Höhner et al. [15] arranged a series of positioning points along the particle boundary, and formed a simple polyhedron model by connecting these points to construct edges and triangular surfaces that effectively modeled various polyhedron shaped particles by controlling the number of triangular surfaces. Ashmawy [16] proposed a technique based on overlapping rigid clusters that can form particles with complicated shapes using only a few overlapping disks to fill a particle domain, which has been used to great effect. Based on fourier analysis, Das et al. [17] provided a new method for building three-dimensional (3D) particles by synthesizing the shape of a two-dimensional (2D) projection of a particle into a 3D shape skeleton, and using spheres to fill out the particle domain. If particles are to be subjected to deformation or fracture, the overlapping displacement between disks must not be too large. Jensen et al. [18–20] simulated particles of various roughness using clusters comprised of disks with various radius, and particles modeled by this method can even be subjected to inelastic deformation under load. Particles modeled by the methods described above are generally configured as ellipsoids or spheres, and, for actual particles with complex roughness and texture, there are greatly difference simulation results often deviate markedly from reality [21]. Moreover, a combination of disks (or spheres) is likely to result in kinematic parameters (such as centroid and moment of inertia) that deviate from the actual conditions, which will also result in unrealistic mechanical properties.

In this paper, the mesoscopic characteristics of particles are considered, and three discrete element cluster modeling techniques are proposed whereby the kinematic parameters are matched with actual values by adjusting the densities of the discrete elements. Lastly, the resulting modeled characteristics of the different methods are verified by a set of experiment of piston movement, and the discrete element cluster modeling methods are discussed.

2 Two-dimensional description of particle shape

Through the analysis of mesoscopic geotechnical particles by the DEM, the shape, roughness, and texture of the surface are key factors that affect macro-mechanical properties. The boundary of particles can be depicted by closed polyline in 2D space, and every polyline can be constituted from a series of points that can be obtained through field measurements, digital image processing, or computerized tomography scans.

PFC is generally used to analyze interactions between particles, which fills the internal region of a particle by discrete elements with different combination forms. To ensure the kinetic geometrical characteristics of particles, the barycentric position of particles must first be determined, and the area, centroid coordinates, inertia moment, and inertia rotation of a particle are subsequently calculated, all of which can be obtained with the aid of constrained Delaunay triangulation [22].

The boundary of a particle is obtained from a digital image or field measurement, as shown in Fig. 1a. When the boundary of an arbitrarily shaped particle is described by polygons, units with smaller control dimensions can be used in constrained delaunay triangulation, as shown in Fig. 1b. From this structure, basic particle information is calculated respectively with the help of the discrete triangles illustrated in Fig. 1c.

The calculation of basic particle information is as follows.

$$\text{Particle area:} \quad S_p = \sum_{i=1}^{N} s_i \tag{1}$$

Here, s_i is the area of triangle i of Delaunay triangulation the mesh.

Particle centroid coordinates:

$$x_p = \left(\sum_{i=1}^{N} s_i x_i \right) \Big/ S_p \tag{2}$$

$$y_p = \left(\sum_{i=1}^{N} s_i y_i \right) \Big/ S_p \tag{3}$$

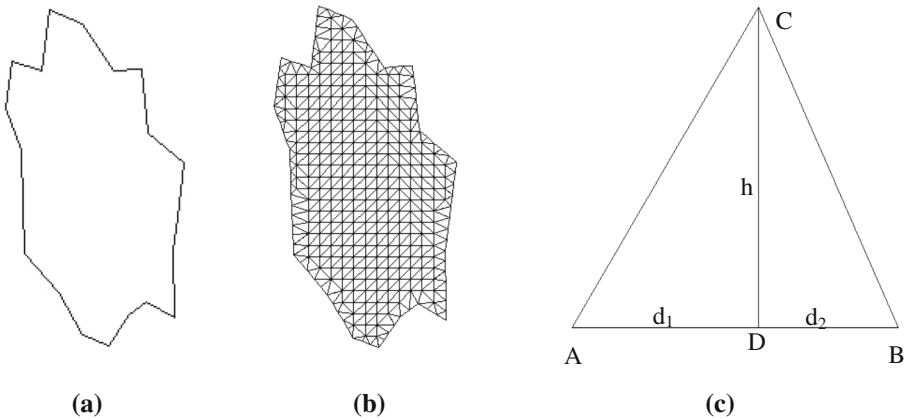

Fig. 1 Calculation of the basic information of an arbitrarily shaped particle. **a** The outline of the particle. **b** The effect drawing of applying Delaunay triangulation. **c** An arbitrary *triangle* of Delaunay triangulation mesh, where the given parameters are used to calculate the inertial moment

Here, x_i is the x coordinate i and y_i is the y coordinate of the centroid of triangle i, respectively.

Mass moment of inertia around the particle centroid:

$$I_p = \sum_{i=1}^{N} \left[s_i (x_i - x_c)^2 + s_i (y_i - y_c)^2 + I_{ti} \right] \tag{4}$$

Here, I_{ti} is the rotational inertia moment of triangle i around the triangle centroid. Taking the triangle in Fig. 1c as an example, its rotational moment of inertia is as follows:

$$I_{\text{ti}} = \left(d_1 h^3 + d_2 h^3 + h d_1^3 + h d_2^3 \right) /36.$$

3 Two-dimensional description of overlapping discrete element clusters

3.1 Modeling rules

To package the region with disks in the particle domain shown in Fig. 1a, and to decrease the number of disks to the smallest number possible, the number of line segments along the particle boundary can be appropriately increased to prevent the length of some segments from being too large. Then, the boundary of the particle can be regard as a polygon, which is made up of N boundary points, as shown in Fig. 2a.

The first disk is applied with its center lying at the centroid of the particle, as shown in Fig. 2b. Meanwhile, the disk must have the largest possible radius without containing any boundary points. This disk is regarded as the first-generation disk.

Regarding the lines connecting boundary points on each side of a given boundary point as vectors, the angular bisector vector of every boundary point is calculated. The center position of the disks is changed along the angular bisector within the particle boundary. At every center position, the radius of disk is increased gradually until a single boundary point is on the disk boundary. Disks with different center position are compared with each other, and the disk having the largest radius is reserved as the largest disk for that boundary point. N disks are then obtained by a cyclic examination of all boundary points, and, from these, the largest among the N disks is selected as the second-generation disk, as shown in Fig. 2c. According to this rule, a single disk will be selected at each iteration until the coverage meets the requirements. A complete filling of the particle domain by disks is illustrated in Fig. 2d, and the generated particle is shown in Fig. 2e.

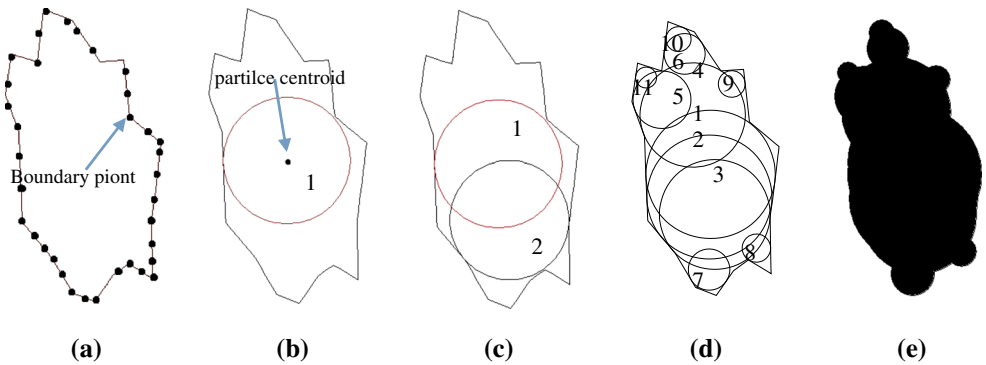

Fig. 2 The particle filling process. **a** Schematic diagram of boundary points along the particle outline. **b** The center of the first disk lies at the position of the particle centroid, and the radius takes its maximum value. **c** The second-generation disk is obtained by an iterative procedure. **d** The particle is completely filled by disks. **e** The generated particle

Usually, the ideal shape of a particle can be achieved with about a dozen disks, and the modeling method is very simple. In addition to controlling the filling process according to the boundary points, the process can also be controlled by the vector normal to each boundary segment, with the advantage that all disks are tangent to the boundary.

The coverage area of the disks should be calculated during the particle filling process. However, it is very difficult to update the coverage area at each iteration because of complex overlapping between new and existing disks. Therefore, Delaunay triangular mesh can be used to evaluate the coverage according to whether or not a triangle centroid is located within a disk. If a triangle centroid lies within a disk, the triangle area belongs to the coverage area, and the coverage area is approximated by summation areas of the triangle located within disks. The obtained approximate coverage area is close to the real value if the size of the Delaunay mesh is sufficiently small.

3.2 Geometrical feature matching of particles

Because of the overlap among disks, a uniform disk density can be estimated on the basis of the total disk area and the particle area.

The estimated uniform disk density is:

$$\rho_{\mathrm{e}} = \rho \cdot \frac{S_p}{\sum_{i=1}^{n} \pi r_i^2} \tag{5}$$

Here, r_i is the radius of disk i (for a total of n disks), ρ is the real particle density, and S_p is the real particle area.

However, to ensure the optimal coverage of a particle, the distribution of disks is uneven, which leads to a variety of parameters such as the position of the center of gravity and the mass moment of inertia, affecting the kinetic characteristics of the particle. Therefore, it is necessary to adjust the density of each disk to accurately represent the real particle.

Firstly, the total disk mass is set equal to the actual mass of the particle.

$$\sum_{i=1}^{n} \rho_i \pi r_i^2 = \rho S_p \tag{6}$$

Secondly, the centroid coordinates of the disk cluster are set to agree with the actual coordinates.

$$\sum_{i=1}^{n} \rho_i \pi r_i^2 (x_i - x_c) = 0 \tag{7}$$

$$\sum_{i=1}^{n} \rho_i \pi r_i^2 (y_i - y_c) = 0 \tag{8}$$

Thirdly, the mass moment of inertia around the centroid of the disk cluster is set to agree with the mass moment of inertia of the particle.

$$\sum_{i=1}^{n} \rho_i \pi r_i^2 \left[(x_i - x_c)^2 + (y_i - y_c)^2 + 0.5 r_i^2 \right] = I_p \tag{9}$$

3.3 Analysis of the matching process for the kinematic parameters of the particle

From the above, four disks selected from the disk cluster are given unknown densities, and the density of the remaining disks is set to ρ_{e} as the known condition. The densities of the four disks are then obtained by solving the matching Eqs. (6–9). If the densities of all four disks are positive, the requirement is met. If not, the mass of disks with calculated density is non-positive is set as two percent of the total matching mass, and the mass of the other disks is reduced in the same proportion. Then, the process is repeated until the relative densities of all disks are >0. Taking the disk cluster shown in Fig. 2d as an example, an analysis of the matching process is shown in the Table 1.

The purpose of the Sect. 3 is making sure that the kinematic parameters of whole cluster of filling particle are the same as the real particle. Compared with Galindo-Torres et al. [23], this method mentioned in this paper modify kinematic parameters(mass, centroid coordinates and mass moment of inertia around the centroid of the disk cluster) of the filling particle by adjusting density of partly disks, so the kinematic parameters of the filling particle will not affect the results of numerical simulation.

As shown in Fig. 2d, the particle domain is filled with disks, and the kinematic parameters of the particle are compared with those generated from different methods in Table 2.

Table 2 shows that, if only the average density is used, the position of the centroid changes significantly while the total mass of the particle remains the same. The deviation of the mass moment of inertia is as great as 23.7 %, and it can be predicted that the kinetic characteristics trajectory of the modeled particle would be widely different from the actual particle. However, these problems can be overcome by adopting the matching rule for kinematic parameters, which parameters are basically identical of real particles.

4 Two-dimensional description of non-overlapping discrete element clusters

A cluster structured by overlapping disks cannot be subjected to deformation or fracture under a loading process. Otherwise, strain energy release causes distortion of the numerical results. Therefore, a new modeling method with a reduced,

Table 1 An example of the matching process for the kinematic parameters of the particle (based on Fig. 2d)

Iteration number	Disk number	Initial relative density	Matching density	Matching mass	Relative mass	Relative density
The first iteration	1	0.47333	7.101985	36335.59	4357.3	0.851648
	11	0.47333	30.00406	13,222.38	1585.6	3.597995
	5	0.47333	−6.648343	−22,163.44	123.8	0.037139
	3	0.47333	−5.063195	−21,204.08	123.8	0.029564
The second iteration	4	0.47333	−2.889376	−25,523.12	174.4882	0.019753
	6	0.47333	1.716308	10365.33	2189.7290	0.362579
	9	0.47333	−4.794166	−5398.52	174.4882	0.154955
	10	0.47333	12.03376	29280.72	6185.7060	2.542195
The third iteration	1	0.85165	0.252937			
	2	0.47333	0.859075			
	9	0.15496	0.814797			
	7	0.43333	2.803048			

Table 2 Comparison of the actual kinematic parameters with those estimated by different methods (based on Fig. 2d)

Property parameter	Actual particle	Average density method	Mass matching method
Area (mm^2)	120,798	120,798	120798
x Coordinate of centroid (mm)	7.645602	8.3928217	7.645602
y Coordinate of centroid (mm)	0.921489	−0.5415063	0.921489
Mass moment of inertia (mm^2)	2.9676E+9	2.263845E+09	2.9677E+09

or zero, superposition of disks is necessary for solution of this problem.

4.1 The distance between points and the boundary

In arbitrary connected domain, the distance between a given point and the domain boundary defines the degree to which the point is nearby the boundary, as shown in Eq. (10):

$$d = \lambda \cdot \min_i \|d\|_{si}\,, \tag{10}$$

where $\|d\|_{si}$ is the distance between the point and the boundary. λ is a flag of within or outside of the boundaries, if the point is within the boundary $\lambda = 1$, then the function value is positive. Otherwise, $\lambda = -1$ it is outside of the boundaries. Union, difference, and intersection can be used when the boundary is a simple combination form, as given by Eq. (11). Where, A and B represent different type segments which constitute of the particle boundary. d_A and d_B respectively represents the distance of the disk center to A type segments and B type segments, as shown in Fig. 3.

$$\begin{cases} d_{A\cup B} = \min(d_A, d_B) \\ d_{A/B} = \max(d_A, -d_B) \\ d_{A\cap B} = \max(d_A, d_B) \end{cases} \tag{11}$$

If this is applied to a particle domain, and the object of interest is a disk of radius r, the following conditions hold.

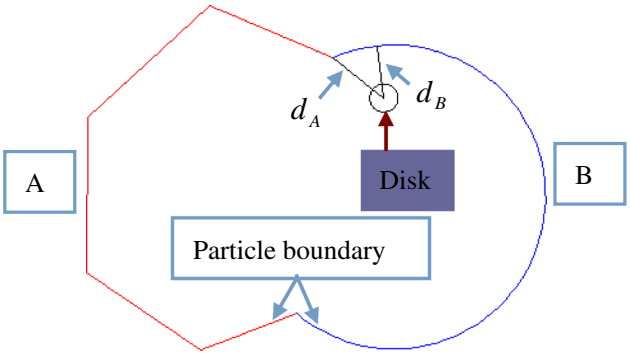

Fig. 3 Different type segments of the particle boundary

When d is greater than r, the disk is located in the particle domain. When d is equal to r, the disk is tangent with the particle boundary. If d is less than r and >0, the disk is the boundary disk. To couple the boundary disk with the boundary, the radius of the boundary disk should be reduced. When d is <0, the disk is outside of the particle boundary, and the disk should be discarded.

4.2 Initial filling point

To ensure filling efficiency, the distance between the center of arbitrary meshes (as shown in Fig. 1b) and the boundary should be calculated firstly. The center of the triangle mesh

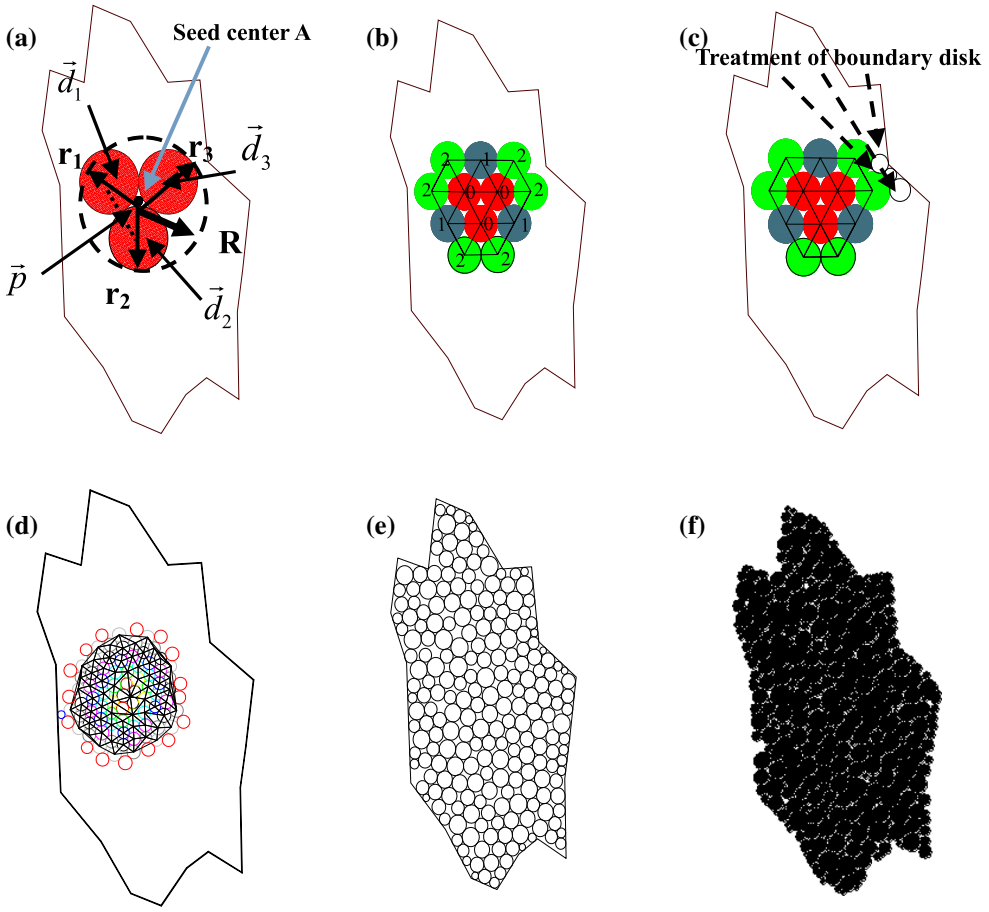

Fig. 4 Building process of a non-overlapping discrete element cluster. **a** The position of the seed based on seed center A. **b** Three generations of disks, where disks with the same color belong to the same generation. Here, the seed is regarded as an algebraic extending center. **c** The treatment of boundary disks once the disks have extended to the boundary location. **d** Local Delaunay mesh inside the front edge of extension. **e** Completion of the filling corresponding process. **f** The resulting particle shape

that has a maximum distance to the boundary is set as the initial filling position of the seed, as shown in Fig. 4a.

For the 2D problem, the initial filling point (known as the seed) consists of three disks that are tangent with each other, and attain the maximum density in the local area. The size of each disk is provided according to the distribution law given by the user, and each disk is located in a given zone in the manner described below. Arbitrarily complex particles can be built up by an expansion filling method, which means new disks are generated around existing disks in the front. The front is then constantly updated, finally a compact particle can be generated [24].

Assuming r_1, r_2 and r_3 are the radius of the three disks which formed the seed as shown in Fig. 4a. The center of the three disks can form a triangle, and the centroid of the triangle is called the seed center A, and the position vector of A can be described as $\vec{p}$. The positions $\vec{d}_1$ and $\vec{d}_2$ of the first and second disks, respectively, can be randomly determined by $\vec{p}$:

$$\vec{d}_1 = \vec{p} + \vec{n} \cdot r_1; \vec{d}_2 = \vec{p} - \vec{n} \cdot r_2, \tag{12}$$

where $\vec{n}$ is a random unit vector. $\vec{d}_3$ is the position of the third disk, which can be determined by the condition of tangency with the first and second disk.

If the center coordinates and radii of two disks are known, the position of a new disk of radius r can be determined for a 2D case. $P_1(x_1, y_1)$ and $P_2(x_2, y_2)$ respectively represent the coordinates of the two known disks, and r_1 and r_2 represent their radii. The position of the new disk $P(x, y)$ can be obtained by solving Eq. (13).

$$\begin{cases} (x - x_1)^2 + (y - y_1)^2 = (r + r_1)^2 \\ (x - x_2)^2 + (y - y_2)^2 = (r + r_2)^2 \end{cases} \tag{13}$$

After solving Eq. (13), it is necessary to test the two roots of the equation. If the new disk is located in the particle domain and does not overlap with other disks, the new disk is accepted.

After the initial position and the radii of the seed disks are known, the smallest circle whose center is located at the initial position with a radius R that covers the three seed disks is defined as seed region. R is defined by Eq. (14).

$$R = \max\left\{\left|\vec{d}_1 - \vec{p}'\right| + r_1;\quad \left|\vec{d}_2 - \vec{p}'\right| + r_2;\quad \left|\vec{d}_3 - \vec{p}'\right| + r_3\right\} \tag{14}$$

4.3 Localized Delaunay triangulation

The positions of the seed and the first three disks are taken as reference points, and the localized Delaunay method is used to generate triangle meshes for 2D cases. Triangles containing the seed position and one side length L_{ij} (the connected line between No.i and No.j vertexes of every triangle) of which satisfy $L_{ij} - r_i - r_j \geq 2R_{\max}$ (where r_i is the radius of disk located at vertex No.i) are discarded, the three vertices of the remaining triangle are used as centers to generate new disks with known radii, as shown in the Fig. 4b. A new disk is judged whether it overlaps with existing disks or the particle boundary, and disks that overlap with existing disks are abandoned. However, if a disk overlaps the particle boundary, its radius and position coordinates are evaluated. If the radius of the disk is in the range $[R_{\min},\ R_{\max}]$, it is accepted. Otherwise, it is abandoned. Repeat this process until no new disks are generated. This process of generating disks is called disk expansion.

From the standpoint of computational efficiency, it is impossible that all disk positions are chosen as reference points for Delaunay triangulation at every expansion process in the sequence of expansion. Therefore, disks that are generated during a given expansion process are equivalently labeled, as shown in Fig. 4b. The disk generation number increases with the expansion sequence, where the disks that compose the seed are defined as generation zero. Disks whose generation number differs from the current generation number within a specified value are denoted as wavefront, and the specified value is defined as the wavefront thickness. There is overlapping between two adjacent wavefronts, the overlapping region can be repeatedly filled when a complex shaped particle is modeled. When the thickness of the wavefront is greater, the probability of repeated filling is higher. While a high filling coverage can be achieved when the wavefront thickness is large, which contributes to satisfying the specified bulk density and size distribution, computational efficiency will certainly be sacrificed.

The radius of a new disk is generated at random or in accordance with the requirements of the user in the advancing process of the wavefront, and, in some places, the new disk may not be ideally placed on the unit of the wavefront. If so, largera void will be generated in the position where the disk cannot be placed. However, for a wavefront with a certain thickness, the larger void may be filled by a subsequent expansion process and the filling density increased.

4.4 Coupling of boundary disks

When the filling region is a polygon, the radius r of a newly generated disk that overlaps with the boundary must satisfy Eq. (15).

$$n_x(x - x_b) + n_y(y - y_b) = r \tag{15}$$

Here, n_x and n_y are the tangent vectors of the boundary edge, and x_b and y_b are the coordinates of a point on the boundary edge.

A disk judged to be a boundary disk is not necessarily tangent with the boundary. Therefore, the restriction of the disk radius is usually reduced to ensure that the boundary disk is tangent with boundary, which can closely couple the disk with the boundary. To ensure that the disk is tangent to the boundary, the proper radius of the disk can be searched by optimization algorithm. Supposing that the radius of a boundary disk is r_0, the undetermined radius is in the range $[0,\ r_0]$. However, for disk radius infinitesimal, the number of disks will be extremely large. A practical method reduces the radius of the boundary disk by a factor k_0, based on the required minimum radius $r_{\min}$. The range of the radius of the boundary disk is $[k_0 r_{\min},\ r_0]$, where k_0 is >0 and <1.0. The coordinate of circle center can be calculated through triangle mesh and known disks. Then, the distance between circle center and a complicated boundary can be obtained as follows:

$$f = \left|d' - r'\right| \tag{16}$$

where d' is the distance between the new generated disk center and the boundary and r' is the trial radius.

4.5 Process of repeated filling

When a particle is modeled using the non-overlapping method, reducing the proportion of disks in a state of imbalance are very necessary in the simulation of materials by DEM.

The particle area is divided into an m × n rectangular grid, the disk centers are extracted in every mesh, and local Delaunay triangulation and the refilling process (filling the space between filled disks) is carried out. To ensure that voids can be filled by disks, the minimum radius of a disk must be less than the required minimum radius. After Delaunay triangulation, the new disks will be generated for meeting the requirement. Once there is a solution, the radius of a disk is gradually enlarged until the new disk is tangent with

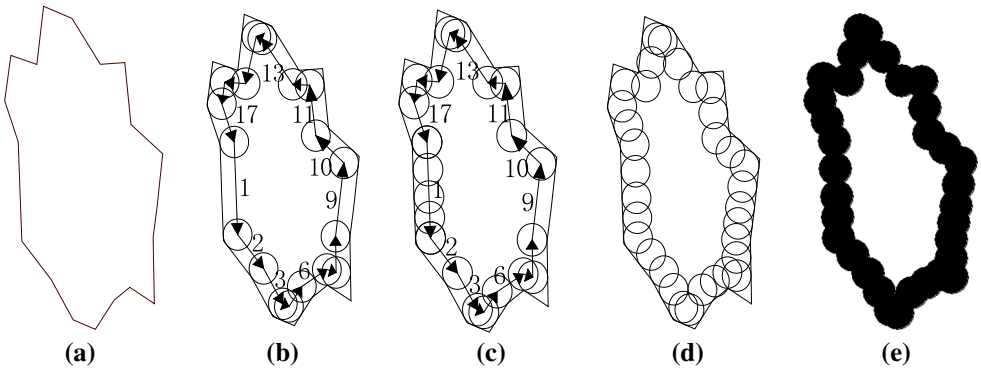

Fig. 5 The process of two-dimensional boundary filing of particles. **a** The boundary of a particle. **b** Disks are filled at the angles of the boundary, and the sections between disks are numbered. **c** Section 1 shown in **b** is completely filled by disks. **d** All sections are completely filled by disks. **e** The completely filled particle boundary

other disks. The above process is repeated for the current disk system, until no new disks are generated.

5 Two-dimensional description of the boundary filling method for discrete element clusters

If the boundary of a particle must be captured with the highest fidelity, disks can be generated only along the inside boundary. This technique ensures that the surface of the particle is more realistic, and is here referred to as the boundary filing discrete element cluster modeling method. However, this method also requires density adjustment according to Eqs. (6–9).

The basic method approach of the boundary filing method is to generate disks at every angle of the particle boundary, as shown in Fig. 5a, and the sections between adjacent disks are numbered, as shown in Fig. 5b. The radius of a filled disk can be adjusted according to the angle and the side length of the boundary to provide the best filling effect. The degree of overlap between disks can be adjusted when locating disks along every section within the range [0, 2R], such that two adjacent disks may be tangent with each other but may also completely coincidence. As shown in Fig. 5c, Sect. 1 is first completely filled with disks, and the remaining sections are filled successively. Figure 5d illustrates the stage of the process where all sections are completely filled by disks, and Fig. 5e illustrates the filled particle boundary.

6 Discussion

The overlapping discrete element cluster technique can use a small number of disks to model a complicated particle, which provides for rapid calculation. However, a large amount of strain energy is released when particle breakagethe simulated is subjected to deformation or fracture, which would provide distorted simulation results. Use of the non-overlapping discrete element cluster technique requires a large number of disks, resulting in a slow calculation speed, but the results will be more realistic when particle breakage deformation or fracture is simulated, even in the absence of kinematic parameter matching. Therefore, the numerical simulation technique should be selected according to the requirements.

To verify the rationality of the above described discrete element cluster modeling methods, the PFC2D particle flow package is used to simulate the laboratory test shown in Fig. 6a. The experimental device is comprised of a wooden container and piston. Motion morphology and position of particles are measured and recorded as the piston moves upward. All rock blocks in the container are numbered from 1 to 68. The particle boundaries are obtained from the digital image. From the obtained boundaries, particle cluster models are constructed according to the overlapping discrete element cluster, non-overlapping discrete element cluster, and boundary filing discrete element cluster modeling method. The numerical models by above three modeling methods are respectively shown in Fig. 6b–d. The matching of kinematic parameters is carried out in the building process of the overlapping discrete element cluster and boundary filing discrete element cluster modeling models. Figure 6b–d demonstrate that all three modeling methods reflect meso characteristicthes of the particles in Fig. 6a reasonably well. In the laboratory test, the piston moves upward at a speed of 0.01 m/s, and the final displacement of the piston is 0.1 m, and these values are applied to the numerical simulations for comparability between the different discrete element cluster modeling methods. When the piston stops, the particle positions of the laboratory and numerical simulation experiments are recorded, as shown in Fig. 6e–h. The numerical simulation results of the three modeling methods are observed to uniformly coincide with the results of the laboratory test.

It can be seen from Table 3 that the overlapping discrete element cluster modeling method executes with a significantly fewer number of disks and two-thirds the number of operational time steps compared with the non-overlapping discrete element cluster modeling method. The boundary discrete element cluster modeling method can be regarded as a particular case of the overlapping discrete element cluster modeling method. Although the number of disks employed

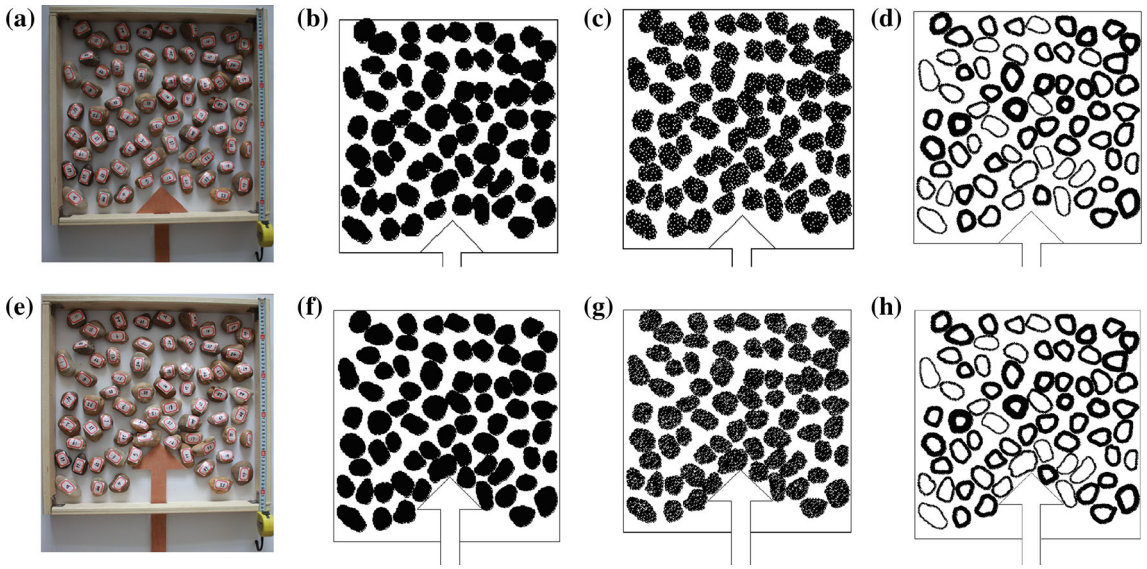

Fig. 6 Comparison between experimental of piston movement and DEM simulations using different discrete element cluster modeling methods. **a**, **e** Photographs of the laboratory test model and results, respectively. According to the particle boundaries shown in **a**, numerical models are built using the overlapping discrete element cluster, non-overlapping discrete element cluster, and boundary filing discrete element cluster modeling methods, as shown **b–d**, respectively, and the simulated results are respectively shown in **f–h**

Table 3 Comparison of the three different discrete element cluster modeling methods

	Number of disks	Operational time steps (ten thousand steps)	Centroid position	Applicable to particle deformation and fracture
Overlapping discrete element cluster	388	400	Equivalent to actual particle centroid	No
Non-overlapping discrete element cluster	3211	1200	Equivalent to actual particle centroid	Yes
Boundary filing discrete element cluster	2731	120	Equivalent to actual particle centroid	No

by the boundary discrete element cluster modeling method is seven times that of the overlapping discrete element cluster modeling method, the operational time steps are reduced by 70 %.

The kinematic parameters matching process ensures that the centroid of the modeled particle coincides with the position of the actual particle centroid for all three modeling methods. While the matching process has little effect upon the non-overlapping discrete element cluster modeling method, deviations from the actual centroid position of 30 % occur for the overlapping and boundary filing discrete element cluster modeling methods without the matching process.

The outline of a 2D particle can be represented by continuous polylines while the outline of a 3D particle can be obtained by a combination of triangles. The 2D filling methods described above can be conveniently generalized to 3D cases. A sphere with maximum radius is firstly filled at the center of gravity of particle through 3D method of Overlapping Discrete Element Cluster, which is similar to construction of 2D Overlapping Discrete Element Cluster. The process of filling disks relies on angles of particle in three-dimensional particle, and the corresponding filling process of three-dimensional particle depends on surfaces of particle boundary. Due to the number of surfaces is numerous, the probability theory can be used to select some surfaces randomly, and spheres are filled through those surfaces. Furthermore, the number of filling sphere can be controlled by the range of radius of sphere and the probability value.

For construction of 3D non-overlapping discrete element cluster, first four spheres are filled at the center of gravity of particle as initial filling point in 2D case, and then new spheres are generated by expansion filling method. When spheres reach the particle boundary, the sphere radius is usually reduced to ensure that the boundary disk is tangent with boundary, which can closely couple the sphere with the boundary. Figure 7 shows graphical depictions of a particle built by the 3D overlapping discrete element cluster and non-overlapping discrete element clusters modeling methods. The contour characteristics of the particle can be well represented

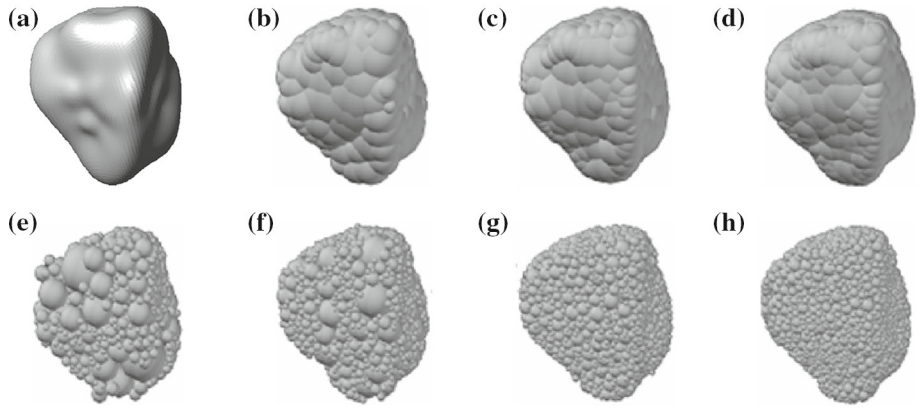

Fig. 7 Modeling methods applied to three-dimensional mesoscopic particles. **a** Is the shape of a real particle. **b–d** Graphical depiction effect drawings of a particle built by the three-dimensional overlapping discrete element cluster modeling method, and the numbers of spheres are respectively 104, 147, and 230 from *left* to *right*. **e–h** Graphical depiction effect drawings of a particle built by the three-dimensional non-overlapping discrete element cluster modeling method, and the numbers of spheres are respectively 636, 1268, 2035, and 5995 from *left* to *right*

with 200–300 spheres in the 3D overlapping discrete element cluster modeling method, while the number of filling spheres increases by a factor of ten if the same aim is achieved using the 3D non-overlapping discrete element cluster modeling method.

7 Conclusions

In terms of mesoscopic geotechnical particles, the overlapping discrete element cluster and non-overlapping discrete element cluster modeling methods, adopting distance control and Delaunay mesh, have been proposed based on the 2D boundary characteristics of a particle. In addition, the boundary discrete element cluster modeling method has been derived from the overlapping discrete element cluster modeling method. The Advantages and disadvantages of these three modeling methods have been discussed, and several conclusions can be obtained as follows.

1. The technique involved with the overlapping discrete element cluster modeling method is simple, it can greatly reduce the required number of disks (in 2D), and can accurately depict particle characteristics such as the particle boundary outline contour. The overlapping discrete element cluster method is characterized by high calculation efficiency, and the centroid position of the modeled particle can be made to coincide with the actual particle centroid position by the kinematic parameters matching procedure, which ensures that the simulation results of moving particles are reasonable. However, the method is limited for simulation of particle deformation and fracture under an applied external force due to the rigid characteristics of the modeled particle.
2. The non-overlapping discrete element cluster modeling method, based on the tangency condition between disks (in 2D), fills the particle domain with disks at a high filling rate using distance control and Delaunay mesh, where the disks are made to couple with adjacent disks or with the boundary. The method is suitable for building particles with arbitrarily connected regions, and can better realize simulations and analyses of the deformation and failure mechanism of complex mesoscopic geomaterials, although the method employs a relatively large number of disks and requires a correspondingly increased calculation time.
3. The boundary filing discrete element cluster modeling method is derived from the overlapping discrete element cluster modeling method. According to the experimental test conducted, the number of operational time steps required for the boundary filing discrete element cluster modeling method is reduced by seventy percent relative to that of the overlapping discrete element cluster modeling method, although the number of disks required is much greater, which therefore demonstrates a much higher efficiency. Particles modeled by this method belong to a rigid cluster, so the method cannot be used to simulate the deformation and fracture processes of particles. However, it can finely simulate surface friction problems between particles.
4. Three modeling methods not only can be used to fill arbitrarily shaped particle, and the applications can be extended further. Other studies have shown that polyhedron can simulate and predict structure form of nano and colloidal structure [25]. More discussions will be made on the applications of the three filling methods in nano, colloidal and proteinic scale systems in the future.

Acknowledgments This research work was partially carried out with financial support from the National Basic Research Program of China (973 Program) (2015CB057903),the National Natural Science Foundation of China (Grant No. 51309089), the National Key Technology R&D Program (Grant No. 2013BAB06B01), the Natural Science Foundation of Jiangsu Province (Grant No. BK20130846) and the Fundamental Research Funds for the Central Universities (2014B04914). We thank LetPub (www.letpub.com) for its linguistic assistance during the preparation of this manuscript.

References

1. Höhner, D., Wirtz, S., Scherer, V.: A numerical study on the influence of particle shape on hopper diskharge within the polyhedral and multi-sphere discrete element method. Powder Technol. **226**, 16–28 (2012)
2. Govender, N., Wilke, D.N., Kok, S., Els, R.: Development of a convex polyhedral discrete element simulation framework for NVIDIA Kepler based GPUs. J. Comput. Appl. Math. **270**, 386–400 (2014)
3. Li, Y., Yong, X., Thornton, C.: A comparison of discrete element simulations and experiments for 'sand piles' composed of spherical particles. Powder Technol. **160**, 219–228 (2005)
4. Zhou, Y.C., Xu, B.H., Yu, A.B., Zulli, P.: An experimental and numerical study of the angle of repose of coarse spheres. Powder Technol. **125**, 45–54 (2002)
5. Matuttis, H.G., Luding, S., Herrmann, H.J.: Discrete element simulations of dense packings and heaps made of spherical and non-spherical particles. Powder Technol. **109**, 278–292 (2000)
6. Sukumaran, B., Ashmawy, A.K.: Influence of inherent particle characteristics on hopper flow rate. Powder Technol. **138**, 46–50 (2003)
7. Latham, J.P., Munjiza, A.: The modelling of particle systems with real shapes. R. Soc. **362**, 1953–1972 (2004)
8. Kačianauskas, R., Tumonis, L., Džiugys, A.: Simulation of the normal impact of randomly shaped quasi-spherical particles. Granul. Matter **16**, 339–347 (2014)
9. Cundall, P.A., Strack, O.D.: A discrete numerical model for granular assemblies. Geotechnique **29**(1), 47–65 (1979)
10. Ferellec, J.-F., McDowell, G.R.: A method to model realistic particle shape and inertia in DEM. Granul. Matter **12**, 459–467 (2010)
11. Eliá š, J.: Simulation of railway ballast using crushable polyhedral particles. Powder Technol. **264**, 458–465 (2014)
12. Askarishahi, M., Salehi, M.-S., Molaei Dehkordi, A.: Numerical investigation on the solid flow pattern in bubbling gas–solid fluidized beds. Powder Technol. **264**, 466–476 (2014)
13. Yun, T., Kim, Y.: Evaluation of particle simulation methods using aggregate angularity and slump tests. Constr. Build. Mater. **66**, 549–566 (2014)
14. Markauskas, D., Kacianauskas, R., Dziugys, A., Navakas, R.: Investigations of adequacy of multi-sphere approximation of elliptical particles for DEM simulations. Granul. Matter **12**(1), 107–123 (2010)
15. Höhner, D., Wirtz, S., Scherer, V.: A study on the in fluence of particle shape and shape approximation on particle mechanics in a rotating drum using the discrete element method. Powder Technol. **253**, 256–265 (2014)
16. Ashmawy, A.K., Sukumaran, B., Hoang, A.V.: Evaluating the influence of particle shape on liquefaction behavior using Discrete Element Method. In: Proceedings of the Thirteenth International Offshore and Polar Engineering Conference (ISOPE 2003) Honolulu, Hawii, May (2003)
17. Das, N., Giordano, P., Barrot, D., et al.: Discrete element modeling and shape characterization of realistic granular shapes. Int. Offshore Polar Eng. Conf. Proc. **2**, 525–532 (2008)
18. Jensen, R., Bosscher, P., Plesha, M., Edil, T.: DEM simulation of granular media-structure interface: effect of surface roughness and particle shape. Int. J. Numer. Anal. Methods Geomech. **23**, 531–547 (1999)
19. Alonso-Marroquin, F.: Spheropolygons: a new method to simulate conservative and dissipative interactions between 2D complex-shaped rigid bodies. EPL Europhys. Lett. **83**(1), 14001 (2008)
20. Phillips, C.L., et al.: Optimal filling of shapes. Phys. Rev. Lett. **108**(19), 198304 (2012)
21. Kruggel-Emden, H., Rickelt, S., Wirtz, S., Scherer, V.: A study on the validity of the multi-sphere discrete element method. Powder Technol. **188**, 153–165 (2008)
22. Liu, Y., Lo, S.H., Guan, Z.Q., Zhang, H.W.: Boundary recovery for 3D Delaunay triangulation. Finite Elem. Anal. Des. **84**, 32–43 (2014)
23. Galindo-Torres, S.A., Munoz, J.D., Alonso-Marroquin, F.: Minkowski-Voronoi diagrams as a method to generate random packings of spheropolygons for the simulation of soils. Phys. Rev. E **82**, 056713 (2010)
24. Bagi, K.: An algorithm to generate random dense arrangements for discrete element simulations of granular assemblies. Granul. Matter **7**(1), 31–43 (2005)
25. Damasceno, P.F., Engel, M., Glotzer, S.C.: Predictive self-assembly of polyhedra into complex structures. Science **337**, 453–457 (2012)